analytical chemistry

Article

pubs.acs.org/ac

Measurement of the $^{240}Pu/^{239}Pu$ Mass Ratio Using a Transition-Edge-Sensor Microcalorimeter for Total Decay Energy Spectroscopy

Andrew S. Hoover,*[,†] Evelyn M. Bond,[†] Mark P. Croce,[†] Terry G. Holesinger,[†] Gerd J. Kunde,[†] Michael W. Rabin,[†] Laura E. Wolfsberg,[†] Douglas A. Bennett,[‡] James P. Hays-Wehle,[‡] Dan R. Schmidt,[‡] Daniel Swetz,[‡] and Joel N. Ullom[‡]

[†]Los Alamos National Laboratory, Los Alamos, New Mexico 87545, United States

[‡]National Institute of Standards and Technology, Boulder, Colorado 80305, United States

ABSTRACT: We have developed a new category of sensor for measurement of the $^{240}Pu/^{239}Pu$ mass ratio from aqueous solution samples with advantages over existing methods. Aqueous solution plutonium samples were evaporated and encapsulated inside of a gold foil absorber, and a superconducting transition-edge-sensor microcalorimeter detector was used to measure the total reaction energy (Q-value) of nuclear decays via heat generated when the energy is thermalized. Since all of the decay energy is contained in the absorber, we measure a single spectral peak for each isotope, resulting in a simple spectral analysis problem with minimal peak overlap. We found that mechanical kneading of the absorber dramatically improves spectral quality by reducing the size of radioactive inclusions within the absorber to scales below 50 nm such that decay products primarily interact with atoms of the host material. Due to the low noise performance of the microcalorimeter detector, energy resolution values of 1 keV fwhm (full width at half-maximum) at 5.5 MeV have been achieved, an order of magnitude improvement over α-spectroscopy with conventional silicon detectors. We measured the $^{240}Pu/^{239}Pu$ mass ratio of two samples and confirmed the results by comparison to mass spectrometry values. These results have implications for future measurements of trace samples of nuclear material.

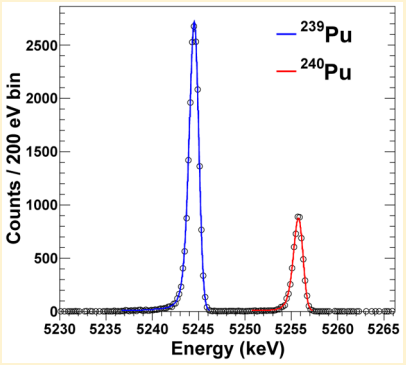

Knowledge of plutonium isotopics, including the $^{240}Pu/^{239}Pu$ mass ratio, is an important component of materials analysis in the context of nuclear nonproliferation, safeguards, and forensics.[1−5] The isotope content carries information about the origin and processing history of the material. Common analysis methods include mass spectrometry and α-spectroscopy. Mass spectrometry is a highly capable method,[6] but one must consider the instrument complexity, cost, and sample preparation requirements. α-Spectroscopy is simple and inexpensive, but sample preparation requires electrodeposition or other methods to achieve thin deposits with minimal energy absorption in the source, and the best silicon detector energy resolution [10 keV fwhm (full width at half-maximum) at 5.5 MeV[7]] is insufficient to resolve closely spaced α-particle line energies, requiring considerable spectral deconvolution.[8,9]

A new approach described here overcomes many of the drawbacks of conventional analysis methods. We use a superconducting transition-edge-sensor (TES)[10] with an attached gold foil to absorb the decay radiation.[11−14] Plutonium isotopes in solution are deposited onto the gold foil and the solvent is allowed to evaporate, then the foil is folded to completely encapsulate the radioactive material. In principle, all decay products are captured in the foil, such that all decays result in a measurement of the single Q-value of the decaying isotope, regardless of the exact decay path. The measurement is insensitive to the fine structure of the daughter nucleus that gives rise to the multiple closely spaced line energies observed in conventional α-spectroscopy. Plutonium α decay directly to the daughter atom ground state produces a ∼5 MeV α-particle and a low-energy (<100 keV) recoil nucleus. For decay to an excited state of the daughter atom, additional radiation of electrons below 100 keV, and X-rays below 20 keV, can be expected from subsequent de-excitation. A gold foil thickness on the order of 15 μm is sufficient to stop practically all of this radiation. Higher-energy electron, X-ray, and γ-ray emissions do occur such that energy can escape the foil, but branching fractions for these decay paths are sufficiently small ($<5 \times 10^{-4}$) that we consider them to be negligible. Measurement of the decay Q-value therefore produces a single spectral peak per isotope.

Decay product energy is thermalized in the gold foil. The TES acts as a sensitive thermometer to measure the temperature rise, which is proportional to the energy deposited. TES microcalorimeters are based on a superconducting film electrically biased in the transition region between the superconducting and normal states. In this narrow transition region, the resistance of the film is strongly dependent on temperature. After the initial temperature rise, the energy flows through a weak thermal link into the heat bath, and the

Received: January 15, 2015
Accepted: February 27, 2015
Published: February 27, 2015

DOI: 10.1021/acs.analchem.5b00195
Anal. Chem. 2015, 87, 3996−4000

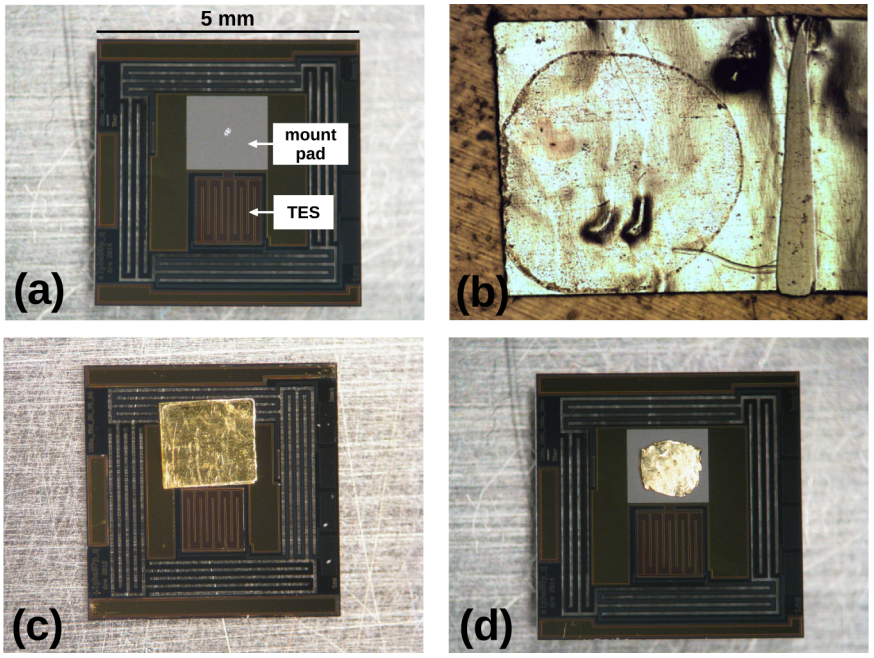

Figure 1. (a) Single detector chip with a small amount of indium powder (used to attach the gold foil) on the mounting pad, (b) a gold foil with visible dried droplet of aqueous solution, (c) a folded gold foil mounted on a detector chip, and (d) a mechanically kneaded gold foil mounted on a detector chip.

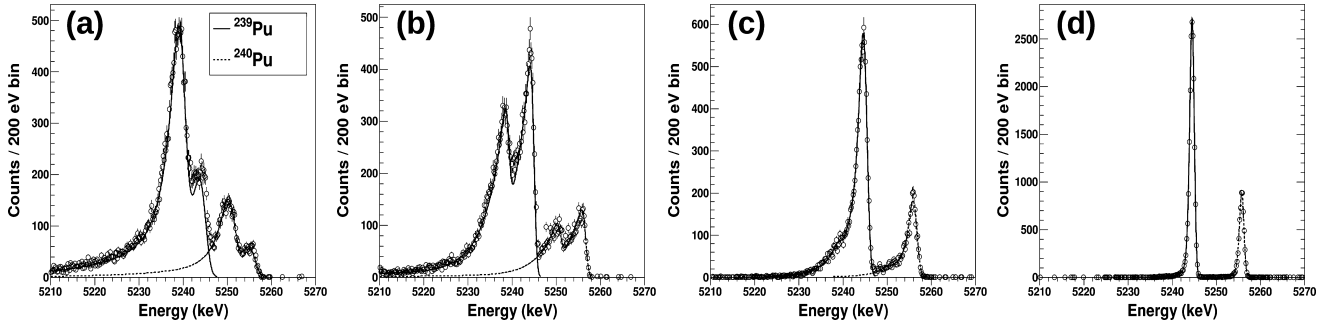

Figure 2. Series of measurements of a $^{240}Pu/^{239}Pu$ sample showing the effects of mechanically kneading the absorber on spectral quality. Lines indicate which counts are associated with each isotope. (a) Unkneaded absorber with two energy peaks visible for each isotope, (b) after absorber was kneaded three times, (c) after absorber was kneaded six times, and (d) after absorber was kneaded 100 times. Mechanically kneading the absorber causes counts to concentrate in the higher-energy peak for each isotope, improves resolution, and reduces low-energy tailing. After kneading 100 times, a single peak is observed for each isotope with high resolution, minimal tailing, and good separation.

temperature returns to its steady-state level until the next event. A voltage bias is applied to the TES so that the current flowing through the TES changes with the increased temperature. This current change is measured using a superconducting quantum interference device (SQUID). A single pulse response is measured for each nuclear decay. Pulses are read out through a single first-stage SQUID, followed by a series-array SQUID, followed by a room-temperature amplifier. The low-noise performance of the TES and SQUID readout allows for very high-resolution measurement of the *Q*-value. Pulse decay time constants are on the order of 30 ms, such that event rates of several counts per second can be realized before pileup of pulses becomes problematic. Our TES devices have a transition temperature around 120 mK, with a transition width of a few millikelvin. Modern refrigeration technology allows for routine operation at these temperatures without any liquid cryogens. Our cryostat utilizes a mechanical helium pulse-tube followed by an adiabatic demagnetization refrigerator.

EXPERIMENTAL SECTION

Conventional devices have used a thin silicon nitride film to support the TES structure.[14] This arrangement is problematic due to the fragility of the membrane and the likelihood of damage during attachment of the gold foil absorber to the TES. Permanent epoxy is often used to attach the absorber to the TES, making removal of the foil impossible after the measurement is complete. We have developed a new style of TES sensor, shown in Figure 1a, to address these problems. The detector chip is fabricated from 275 μm thick silicon. A Mo/Cu TES and bismuth mounting pad are located on the center island. Serpentine legs connect the center island to the frame providing weak conductance to the thermal bath and are a mechanically robust alternative to conventional silicon nitride membrane devices. Each leg has a width of 100 μm and length of 10.55 mm. Total thermal conductance of all the legs together is about 4 nW/K. This design can withstand considerable physical manipulation, repeated absorber attachments, and

DOI: 10.1021/acs.analchem.5b00195
Anal. Chem. 2015, 87, 3996−4000

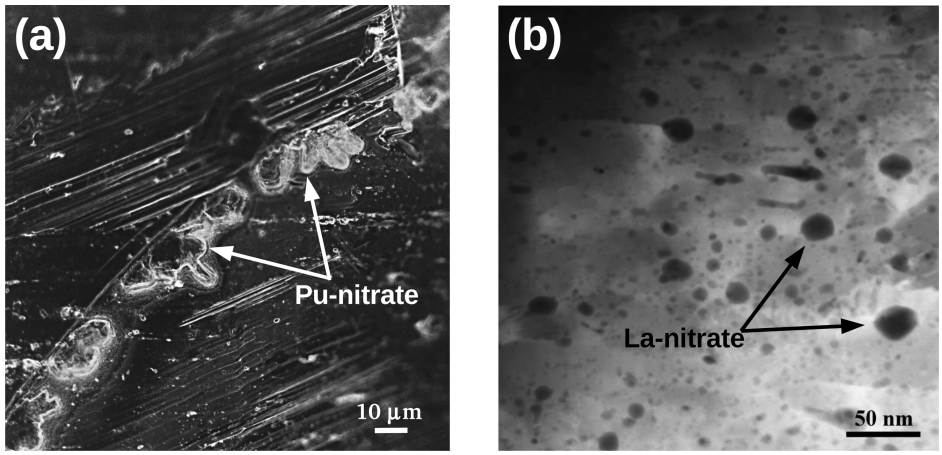

Figure 3. (a) Optical image of plutonium nitrate sample material observed on the surface of the gold absorber foil after droplet evaporation. Typical crystal sizes of 5−10 μm are observed. (b) STEM HAADF-mode image of lanthanum nitrate sample after the absorber was mechanically kneaded, where the dark spots were identified as lanthanum by energy-dispersive X-ray spectroscopy (EDS), showing smaller particle sizes below 50 nm and good integration with the gold matrix.

repeated wire-bond attachments (two wire-bonds are needed to provide the bias current to the TES).

Nominal absorber foil dimensions are 1.8 mm × 3.6 mm × 15 μm, with a total heat capacity of 600 pJ/K. Sample material in solution is transferred to the foil by microsyringe. Figure 1b shows a dried sample on the gold foil. Figure 1c shows a folded gold foil attached to a TES chip using a small amount of indium powder, which has natural adhesive properties. Use of the indium powder allows the foil to be removed from and reattached to the TES any number of times. Thus, the sample can be reacquired for additional analysis and a single TES detector can be used for the measurement of many samples.

An additional sample preparation step is necessary to achieve clean, high-resolution spectra. The absorber foil is mechanically kneaded in order to break up crystalline residue left behind after the sample solution evaporates. The absorber was squeezed multiple times between the jaws of a pliers. Figure 1d shows a kneaded absorber attached to a TES detector. A dramatic effect is observed in the measured energy spectrum as a result of the mechanical kneading (Figure 2). Data collected from an unkneaded absorber show two distinct spectral peaks for each isotope and considerable low-energy tailing. As subsequent rounds of mechanical kneading are applied, counts systematically shift into the higher-energy peak for each isotope, the low-energy tails are reduced, and the resolution improves. After kneading the absorber about 100 times, a very clean spectrum was measured with a single peak at the Q-value of each isotope. For these measurements, the kneaded absorber was formed into a cylinder approximately 1 mm in diameter by 100 μm thick.

We hypothesize that because α-particles deposit the bulk of their energy near the end of their track, events can be considered to occur primarily either in the gold or in the crystalline residue. Due to differing lattice damage effects[15] and thermal transport properties, two energy peaks are observed depending on which material the α-particle primarily interacts with. Mechanical kneading breaks down the plutonium nitrate residue left on the surface of the gold foil after evaporation and improves integration of the radioactive material with the absorber so that most interactions occur directly in the gold, and the secondary peak is eliminated. Figure 3a shows an optical image of a dried plutonium nitrate sample, where crystalline material deposits on the order of 5−10 μm are visible on the surface of the foil. Figure 3b shows a scanning transmission electron microscope (STEM) image of a mechanically kneaded absorber using high-angle annular dark field (HAADF) mode to show atomic number contrast. For the STEM image, lanthanum nitrate was used as a nonradioactive substitute for plutonium nitrate. In the kneaded absorber, the sample material particles are less than 50 nm in size and well-integrated with the gold matrix.

Separate Q-value measurements performed on an electrodeposited ^{238}Pu sample did not show the secondary peak. Furthermore, data collected from dried droplet ^{209}Po and ^{210}Po samples do not show the secondary peak, and polonium is known to autodeposit onto surfaces, leading to the sample being well-adhered to the gold foil rather than inside the residue. Even in an ideal case, some resolution degradation and low-energy tailing is expected from lattice damage effects.[14] Attempts to anneal the absorber with heat and pressure, instead of mechanical kneading, were unsuccessful.

Two samples were prepared for quantitative analysis, hereafter referred to as samples A and B. Starting with ^{239}Pu and ^{240}Pu in 3 M HNO_3 solution obtained from Eckert & Ziegler, the isotopes were mixed and concentrated to produce two samples with low and high ^{240}Pu/^{239}Pu activity ratios and appropriate count rates. The solutions were transferred to gold foils using a microsyringe with microcontroller and allowed to dry. The foils were then mechanically kneaded as described above and mounted to TES detector chips using the indium powder bonding method. Finally, aluminum wire bonds were attached to provide the TES detector bias and signal readout. Cool down of the sample from room temperature takes about 16 h. Pulses were collected for a period of 21.4 h at a rate of about 1 count/s. Counting time is limited by the hold time of the cryostat at the TES transition temperature. Hold times as long as 36 h have been achieved in our cryostat. Significantly longer hold times, and shorter cool-down times, could be realized through the use of alternative cryostat technologies. From the observed count rates the estimated amount of plutonium deposited in the foil is in the range of tens to hundreds of picograms. Cuts were applied to reject pulse records with abnormal pretrigger baseline level or baseline noise, events with pulse pileup, and other spurious events. A

DOI: 10.1021/acs.analchem.5b00195
Anal. Chem. 2015, 87, 3996−4000

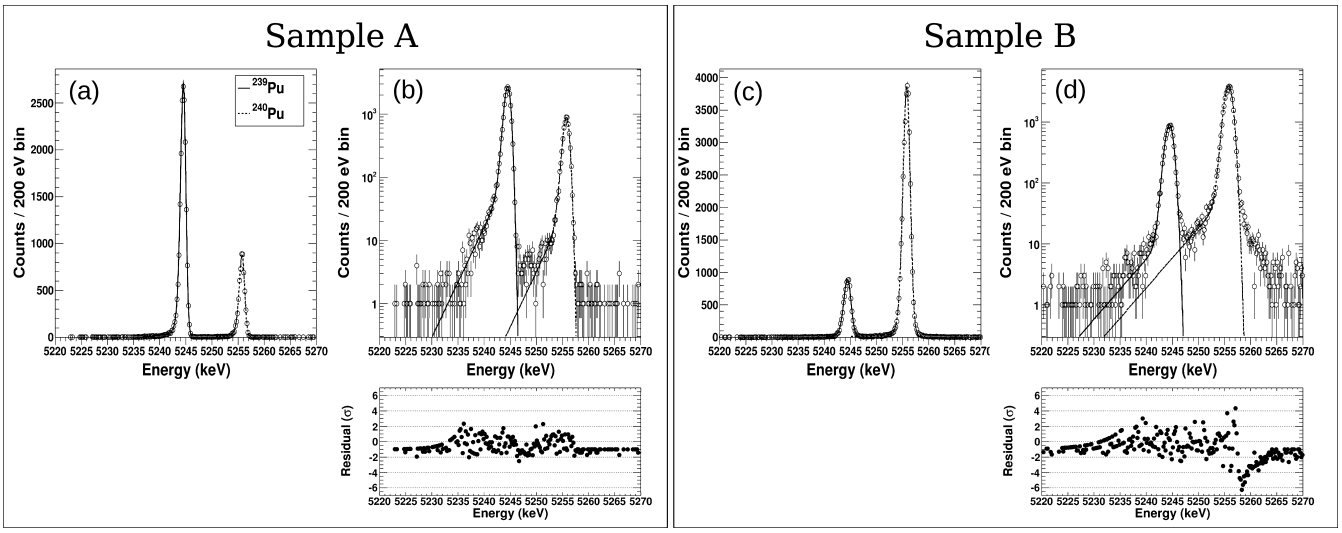

Figure 4. *Q*-value spectra measured for two samples containing different mass ratios of ^{239}Pu and ^{240}Pu. Data are shown on linear and logarithmic scales for samples A (a and b) and B (c and d). Lines show the contribution of each isotope determined by fitting the data with a two-tail Bortels function. Fit residuals (number of σ deviation) are shown below the logarithmic plots for each sample.

Wiener optimal filter was applied to the pulse records to achieve the best resolution.[16] Gain drift on the order of a few tenths of percent can occur during the course of the data collection period. This was corrected for by applying a running-lines smoother to the scatter plot of filtered peak amplitude versus time. A two-point energy calibration is applied to the optimal filtered spectrum using the ^{239}Pu and ^{240}Pu *Q*-values (5244.43 and 5255.75 keV).

RESULTS AND DISCUSSION

The measured *Q*-value spectra for the two samples are shown in Figure 4 on linear and logarithmic scales. We observe nearly complete separation of the ^{239}Pu and ^{240}Pu *Q*-value peaks, only 11 keV apart, with only a small fraction of the ^{240}Pu low-energy tail falling underneath the ^{239}Pu peak. Quantitative spectral analysis was performed by least-squares fitting of the data with a two-tail Bortels function[17] (a Gaussian with two exponential tail components). The spectral fit uses nine free parameters: an overall normalization factor, the ^{240}Pu/^{239}Pu activity ratio, a Gaussian width for each peak, the centroid value of the two Gaussians, two tail parameters shared by each peak, and the intensity of the tail relative to the Gaussian. The ^{240}Pu/^{239}Pu activity ratio (R_{act}) extracted from the spectral fit is converted to a mass ratio using $R_{mass} = R_{act}[(T_{1/2}^{240}M^{240})/(T_{1/2}^{239}M^{239})]$, where $T_{1/2}^{239}$ = 24 110 years is the ^{239} Pu half-life, $T_{1/2}^{240}$ = 6561 years is the ^{240}Pu half-life, M^{239} = 239 is the ^{239}Pu atomic mass, and M^{240} = 240 is the ^{240}Pu atomic mass. In addition to the microcalorimeter *Q*-value measurements, the sample materials were also analyzed by thermal ionization mass spectrometry (TIMS) to provide confirmation of the results.

Table 1 shows a summary of the measurement results. Energy resolutions determined from the Gaussian component of the Bortels fit are as low at 1.0 keV fwhm, an order of magnitude better than typically achieved for α-spectroscopy using conventional silicon detectors. The reduced χ^2 values of the Bortels fit are small, although sample B displays some counts in excess of the fit function for energies above the ^{240}Pu *Q*-value. We observe small pulses (on the order of 10 keV) in the data, which could coincide with the large *Q*-value pulses and escape our algorithm to detect and discard such events.

Table 1. Summary of ^{240}Pu/^{239}Pu Mass Ratio Measurements[a]

sample	TIMS ^{240}Pu/^{239}Pu mass ratio	*Q*-spec. ^{240}Pu/^{239}Pu mass ratio	fwhm (keV)	fit χ_r^2
A	0.08690(45)	0.0884(13)	1.0	1.2
B	1.2053(15)	1.212(15)	1.5	3.4

[a]The TIMS and *Q*-value spectroscopy results are shown with absolute errors in parentheses (coverage factor k = 1). The fwhm of the Gaussian component of the Bortels function fit and the fit reduced χ^2 are shown for the *Q*-value spectral analysis.

These could be events that occur very near the surface of the absorber, such that the α particle can escape, carrying with it the bulk of the decay energy. The rate of the small pulses exceeds the rate measured from natural background sources. The ^{240}Pu/^{239}Pu mass ratio determined by the *Q*-value spectral analysis agrees with the TIMS results within the 1σ statistical error bars. From 21.4 h of data at approximately 1 count/s event rate, statistical errors on the mass ratios in the range of 1.2−1.5% were achieved from the *Q*-value measurements. The Bortels function spectral fit was used due to the small incursion of the ^{240}Pu tail under the ^{239}Pu peak. If the mass ratio were determined by simply summing spectral counts within two regions of interest surrounding the two peaks, we estimate that the result would be subject to an error due to the ^{240}Pu tail as large as 2.4% for sample B, but less than 0.1% for sample A.

CONCLUSIONS

We have developed new instrumentation and methods for measurement of the ^{240}Pu/^{239}Pu mass ratio for samples from aqueous solution. The method has several advantages over conventional approaches such as mass spectrometry and α-spectroscopy. The sample preparation requirements are simple and practical. Droplet evaporation, followed by mechanical kneading of the foil, produces *Q*-value spectra with energy resolution near 1 keV fwhm at 5.5 MeV. Mechanical kneading of the absorber reduces the size of radioactive inclusions within the absorber to scales below 50 nm such that decay products primarily interact with atoms of the host material. The spectra present a single peak per isotope at the decay *Q*-value, rather

DOI: 10.1021/acs.analchem.5b00195
Anal. Chem. 2015, 87, 3996−4000

than multiple peaks observed with conventional α-spectroscopy. This permits a much simpler spectral analysis that is less susceptible to systematic errors from peak deconvolution. Since the detection efficiency is 1, and counts are concentrated into a single peak per isotope, detection sensitivities are expected to be lower than α-spectroscopy limits. The method is still radiometric, with detection sensitivity dependent on isotope half-lives. Looking beyond ^{240}Pu and ^{239}Pu, Q-value spectroscopy could measure isotopes of multiple elements (Pu, Cm, Am, Th, etc.) simultaneously, where mass spectrometry can have difficulties with certain isobars (e.g., ^{241}Pu/^{241}Am, ^{238}Pu/^{238}U), requiring radiochemical separations. After the Q-value measurement, the sample remains in the absorber and could be recovered for subsequent analysis by complementary methods. We believe the method can be extended to the analysis of single plutonium particles, and we are pursuing research on that topic.

AUTHOR INFORMATION

Corresponding Author

*E-mail: ahoover@lanl.gov.

Notes

The authors declare no competing financial interest.

ACKNOWLEDGMENTS

This work was supported by the National Nuclear Security Administration Office of Defense Nuclear Nonproliferation.

REFERENCES

(1) Bellucci, J.; Simonetti, A.; Wallace, C.; Koeman, E.; Burns, P. *Anal. Chem.* **2013**, *85*, 4195−4198.
(2) Ranebo, Y.; Niagolova, N.; Erdmann, N.; Eriksson, M.; Tamborini, G.; Betti, M. *Anal. Chem.* **2010**, *82*, 4055−4062.
(3) Shinonaga, T.; Donojue, D.; Aigner, H.; Bürger, S.; Klose, D.; Kärkelä, T.; Zilliacus, R.; Auvinen, A.; Marie, O.; Pointurier, F. *Anal. Chem.* **2013**, *85*, 4195−4198.
(4) Mayer, K.; Wallenius, M.; Fanghänel, T. *J. Alloys Comp.* **2007**, *444*−*445*, 50−56.
(5) Jakopič, R.; Richter, S.; Kühn, H.; Aregbe, Y. *J. Anal. At. Spectrom.* **2010**, *25*, 815−821.
(6) Becker, J. *Spectrochim. Acta, Part B* **2003**, *58*, 1757−1784.
(7) Knoll, G. *Radiation Detection and Measurement*, 3rd ed.; John Wiley and Sons: New York, 2000; p 393.
(8) Aggarwal, S.; Alamelu, D. *J. Alloys Compd.* **2007**, *444*−*445*, 656−659.
(9) Pöllänen, R.; Siiskonen, T.; Ihantola, S.; Toivonen, H.; Pelikan, A.; Inn, K.; Rosa, J. L.; Bene, B. *Appl. Radiat. Isot.* **2012**, *70*, 733−739.
(10) Irwin, K.; Hilton, G. Topics in Applied Physics. In *Cryogenic Particle Detection*; Enss, C., Ed.; Springer-Verlag: Berlin, Germany, 2005; Vol. *99*, pp 63−149.
(11) Lee, S.; Lee, M.; Jang, Y.; Kim, I.; Kim, S.; Lee, J.; Lee, K.; Lee, Y.; Kim, Y. *J. Phys. G: Nucl. Part. Phys.* **2010**, *37*, 055103.
(12) Yang, Y.; Kim, G.; Kim, K.; Kim, M.; Lee, H.; Lee, J.; Lee, K.; Lee, M.; Lee, S.; Ri, H.; Yoon, W.; Yuryev, Y.; Kim, Y. *Appl. Radiat. Isot.* **2012**, *70*, 2255−2259.
(13) Croce, M.; Bond, E.; Hoover, A.; Kunde, G.; Moody, W.; Rabin, M.; Bennett, D.; Hays-Wehle, J.; Kotsubo, V.; Schmidt, D.; Ullom, J. *J. Low Temp. Phys.* **2014**, *176*, 1009−1014.
(14) Koehler, K.; Bennett, D.; Bond, E.; Croce, M.; Dry, D.; Horansky, R.; Kotsubo, V.; Moody, W.; Rabin, M.; Schmidt, D.; Ullom, J.; Vale, L. *IEEE Trans. Nucl. Sci.* **2013**, *60*, 624−629.
(15) Horansky, R.; Stiehl, G.; Beall, J.; Irwin, K.; Plionis, A.; Rabin, M.; Ullom, J. *J. Appl. Phys.* **2010**, *107*, 044512.
(16) Szymkowiak, A.; Kelley, R.; Moseley, S.; Stahle, C. *J. Low Temp. Phys.* **1993**, *93*, 281.
(17) Bortels, G.; Collaers, P. *Appl. Radiat. Isot.* **1987**, *38*, 831−837.

DOI: 10.1021/acs.analchem.5b00195
Anal. Chem. 2015, 87, 3996−4000